

Affinity and Kinetics of Sialyl Lewis-X and Core-2 Based Oligosaccharides Binding to L- and P-Selectin[†]

Mark E. Beauharnois,[‡] Kevin C. Lindquist,[§] Dhananjay Marathe,[‡] Peter Vanderslice,[⊥] Jie Xia,^{||} Khushi L. Matta,^{||} and Sriram Neelamegham^{*:‡}

Department of Chemical and Biological Engineering, State University of New York, Buffalo, New York 14260, Biacore, Inc., Piscataway, New Jersey 08854, Department of Cancer Biology, Roswell Park Cancer Institute, Buffalo, New York 14263, and Department of Molecular Pharmacology, Encysive Pharmaceuticals Inc., Houston, Texas 77030

Received April 18, 2005; Revised Manuscript Received May 18, 2005

ABSTRACT: Soluble oligosaccharide mimetics of natural selectin ligands act as competitive inhibitors of leukocyte adhesion in models of inflammation. We quantified the binding of simple oligosaccharides based on sialyl Lewis-X (sLe^X) and complex molecules with the core-2 structure to L- and P-selectin, under both static and fluid flow conditions. Isolated human neutrophils were employed to mimic the physiological valency of selectins and selectin ligands. Surface plasmon resonance studies quantified binding kinetics. We observed the following: (i) The functional group at the anomeric position of carbohydrates plays an important role during selectin recognition, since sLe^X and sialyl Lewis-a (sLe^a) were ~5–7-fold poorer inhibitors of L-selectin mediated cell adhesion compared to their methyl glycosides. (ii) Despite their homology to physiological glycans, the putative carbohydrate epitopes of GlyCAM-1 and PSGL-1 bound selectins with low affinity comparable to that of sLe^X-selectin interactions. Thus, besides the carbohydrate portion, the protein core of GlyCAM-1 or the presentation of carbohydrates in clusters on this glycoprotein may contribute to selectin recognition. (iii) A compound Galβ1,4(Fucα1,3)GlcNAcβ1,6-(GalNAcβ1,3)GalNAcα-OMe was identified which blocked L- and P-selectin binding at 30–100-fold lower doses than sLe^X. (iv) Surface plasmon resonance experiments determined that an sLe^X analogue (TBC1269) competitively inhibited, via steric/allosteric mechanisms, the binding of two anti-P-selectin function blocking antibodies that recognized different epitopes of P-selectin. (v) TBC1269 bound P-selectin via both calcium-dependent and -independent mechanisms, with K_D of ~111.4 μM. The measured on- and off-rates were high ($k_{off} > 3 \text{ s}^{-1}$, $k_{on} > 27\,000 \text{ M}^{-1} \text{ s}^{-1}$). Similar binding kinetics are expected for sLe^X-selectin interactions. Taken together, our study provides new insight into the kinetics and mechanisms of carbohydrate interaction with selectins.

Members of the selectin family of adhesion molecules (L-, E-, and P-selectin) mediate one of the first steps that lead to the capture of leukocytes on vascular endothelial cells during normal immune response and inflammation (1). These molecules also regulate lymphocyte trafficking (2), and mediate the formation of heterotypic platelet-leukocyte aggregates in circulation (3).

All three selectins bear C-type lectin domains that recognize a plethora of simple and complex carbohydrates containing sialylated, sulfated, and/or fucosylated sequences in a calcium-dependent manner (3–5). A large number of selectin ligands identified to date, including P-selectin glycoprotein ligand-1 (PSGL-1¹) and glycosylation dependent cell adhesion molecule-1 (GlyCAM-1), express O-linked carbohydrate structures displayed on the core-2 trisaccharide

structure, GlcNAcβ1–6(Galβ1–3)GalNAcα (3). In support of the importance of core-2 based molecules in forming physiologically relevant selectin-ligands, mice with targeted deletion of an enzyme core-2 GlcNAcT-I (β1,6-N-acetylglucosaminyltransferase), which is important for the formation of such glycans, also display reduced binding to E- and P-selectin (6–8). In the case of PSGL-1, it is suggested that sialyl-Lewis^X (sLe^X, NeuAcα2–3Galβ1–4(Fucα1–3)-GlcNAc) may be expressed at the nonreducing terminus of core-2 glycans and that these may represent physiologically important selectin ligands (9, 10). An isomer of sLe^X, sialyl-Lewis^a (sLe^a, NeuAcα2–3Galβ1–3(Fucα1–4)GlcNAc), has also been shown to bind selectins (11, 12). Finally, 6-sulfo sialyl-Lewis^X (NeuAcα2–3Galβ1–4(Fucα1–3)(SE-6)GlcNAc) contained on core-2 structures has been shown to play an important role during L-selectin mediated lymphocyte homing (13).

[†] This work was supported by NIH Research Grants HL63014 (S.N.), HL76211 (S.N.), and CA35329 (K.L.M.). M.E.B. was supported by an American Heart Association predoctoral fellowship (0110106T) and NSF-IGERT grant (0114330) during the course of this work.

* To whom correspondence should be addressed. Phone: (716) 645-2911, ext 2220. Fax: (716) 645-3822. E-mail: neel@eng.buffalo.edu.

[‡] State University of New York, Buffalo.

[§] Biacore, Inc.

^{||} Roswell Park Cancer Institute.

[⊥] Encysive Pharmaceuticals Inc.

¹ Abbreviations: PSGL-1, P-selectin glycoprotein ligand-1; GlyCAM-1, glycosylation-dependent cell adhesion molecule-1; sLe^X, sialyl Lewis-X; sLe^a, sialyl Lewis-a; core-2 structure, GlcNAcβ1–6(Galβ1–3)GalNAcα; Gal, galactose; Fuc, fucose; Man, mannose; NeuAc, sialic acid; GlcNAc, N-acetylglucosamine; GalNAc, N-acetylglucosamine; SE, sulfate ester; Me, methyl; fMLP, formyl peptide.

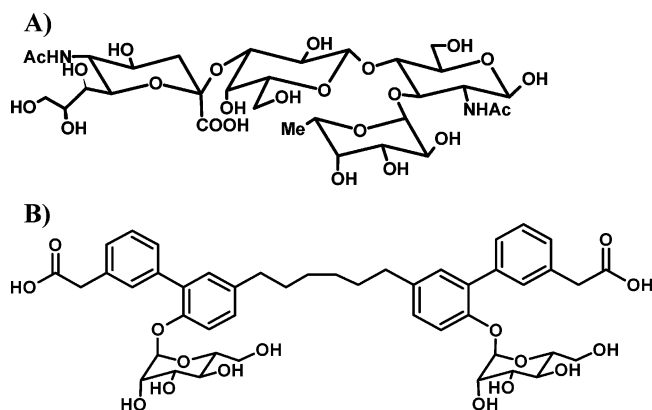


FIGURE 1: Chemical structures. (A) Sialyl Lewis-X. (B) TBC1269.

Soluble molecules designed to mimic the carbohydrate structures of natural selectin ligands can act as effective, competitive inhibitors of selectin mediated cell adhesion *in vivo*. One such molecule, sLe^X, has been shown to reduce tissue injury following ischemia reperfusion (14, 15). Mimetics of sLe^X have also been designed on the basis of diverse approaches (5, 16), including multimeric displays to enhance binding efficacies, as well as approaches involving the replacement of glycosidic linkages with more stable chemical bonds without reducing the mimetics' activity. Among these molecules, a di-sLe^X molecule (TBC1269 or BIMOSIAMOSE) has been designed to utilize mannose and carboxylic acid groups to replace the critical fucose and sialic acid groups of sLe^X, respectively, and a biphenyl group to substitute for the lactosamine core (17, 18) (Figure 1). This molecule has been shown to bind all three selectins to varying degrees (17) and to reduce the number of neutrophils rolling on P-selectin *in vitro* (19). TBC1269 is in phase 2 clinical trials for the treatment of asthma and psoriasis. Non-sLe^X based heparin sulfates, as well as modified heparin structures, have also been shown to block selectin mediated cell adhesion (20, 21). Finally, selectin inhibitors designed on the basis of the core-2 structure display severalfold greater blocking function compared to sLe^X (22).

In the current paper, we tested the possibility that synthetic carbohydrates based on the exact structures of natural glycans expressed on PSGL-1 and GlyCAM-1 can be superior inhibitors of selectin binding. In addition to binding studies under static conditions, experiments were also conducted under physiologically relevant fluid flow conditions. Isolated human neutrophils were used in many assays in order to closely mimic the natural valency of selectins and their ligands, since this feature may affect selectin–ligand recognition specificity (23). Surface plasmon resonance studies were performed to directly measure the affinities and kinetics of selectin–carbohydrate interactions. Our studies suggest that the protein core of GlyCAM-1 or the presentation of carbohydrates in clusters on this glycoprotein may contribute to selectin recognition. They identify a novel molecule Gal β 1,4(Fuc α 1,3)GlcNAc β 1,6(GalNAc β 1,3)GalNAc α -OMe which blocked L- and P-selectin binding at 30–100-fold lower doses than sLe^X. This molecule may represent a candidate for future drug development. Finally, in the first measurements of the affinity and kinetics of selectin interaction with carbohydrates, we observed that an sLe^X mimetic (TBC1269) bound P-selectin with a dissociation constant (K_D) of \sim 111.4

μ M, and very rapid association and dissociation rates ($k_{off} > 3 \text{ s}^{-1}$ and $k_{on} > 27\,000 \text{ M}^{-1} \text{ s}^{-1}$).

MATERIALS AND METHODS

Materials. All monoclonal antibodies (mAbs) were from mouse hosts unless otherwise noted. Adhesion blocking mAbs against PSGL-1 (clone PL1, IgG1) and P-selectin (G1, IgG1) were purchased from Ancell (Bayport, MN). P-Selectin blocking antibody humanized EP5C7 was kindly provided by Protein Design Labs. Anti-L-selectin (DREG-56, IgG1), anti-CD11a (clone TS1/22, IgG1), and anti-CD18 (clone IB4, IgG2a) antibodies were purified from hybridoma cultured in serum-free media (ATCC, Manassas, VA). Blocking mAbs were used at 10 μ g/mL in all runs unless otherwise noted. All secondary antibodies were from Jackson ImmunoResearch Labs (West Grove, PA), isotype match control reagents for flow cytometry runs were from Becton Dickinson (San Diego, CA), and chemicals were from Sigma (St. Louis, MO) unless otherwise noted.

The selectin inhibitors tested during the course of this study are listed in Table 1 along with references that describe the synthesis scheme and characterization for each compound. The concentration of these compounds was varied in each assay as discussed in Results.

Most studies that assayed “L- and P-selectin chimera static binding” (described below) used human L- and P-selectin fusion proteins produced in Chinese hamster ovary (CHO) cells from GlycoTech (Gaithersburg, MD). These molecules consist of the lectin domain, the EGF domain, and most of the short consensus repeat domains (2 for L-selectin and 9 for P-selectin) of human selectin fused to a human IgG1 tail (24). In a few cases, the P-selectin fusion protein used was from a baculovirus expression system that is described next.

All “surface plasmon resonance” runs employed a chimeric P-selectin fusion protein that was produced using the Bac-to-Bac baculovirus expression system from Invitrogen Life Technologies (Carlsbad, CA). Briefly, recombinant DNA encoding the fusion protein was cloned into pFASTBac-1 plasmid and transformed into DH10Bac *Escherichia coli* cells. Recombinant bacmid DNA was purified from the DH10Bac cells and used to transfect SF21 insect cells. After three rounds of amplification, high titer virus was used to infect SF21 cells for protein production. The cells were grown in EX-CELL 405 serum-free growth media (JRH Biosciences, Lenexa, KS). Protein was purified from the cell supernatants using protein G Sepharose (Pharmacia) in some cases. The P-selectin-IgG chimera produced consists of the first 158 amino acids of the mature protein including the lectin and EGF domains fused to a 220 amino acid sequence that encodes the mouse IgG2a Fc portion. This selectin is dimeric and had a molecular weight of \sim 120 kDa when run under nonreducing conditions, and \sim 50 kDa when run under reducing conditions using SDS–PAGE.

Neutrophil Isolation. Blood was collected from healthy, nonsmoking volunteers by venipuncture into a sterile syringe containing 10 units of heparin (Elkin-Sinn Inc., Cherry Hill, NJ)/mL of blood. Polymorphonuclear cells were isolated as previously described (25). The percentage of neutrophils in this fraction was $>90\%$, and the viability measured by trypan blue exclusion was $>99\%$. Neutrophils isolated using this protocol were kept at 4 $^{\circ}$ C in a Ca²⁺-free HEPES buffer until use, typically within 2 h of isolation.

Homotypic Neutrophil Aggregation. The ability of our compounds to block L-selectin mediated cell adhesion under fluid shear conditions was studied in experiments that measured neutrophil homotypic adhesion rates (25, 26). These runs were performed using a VT550 cone-plate viscometer (Haake Inc., Paramus, NJ) equipped with a 2° cone. Briefly, 50 μL samples containing 0.5×10^6 neutrophils/mL in HEPES buffer containing 1.5 mM Ca^{2+} and 0.1% human serum albumin (Bayer Corporation, Elkhart, IN) were incubated with or without the cell-adhesion blocking reagent for 7 min at room temperature (RT) and 3 min at 37 °C prior to being placed in the gap between the cone and the plate of the viscometer. Cells were then stimulated with 1 μM formyl peptide (fMLP), and fluid shear was immediately applied at a shear rate of 1500 s^{-1} to the cell suspension by rotation of the cone. Ten microliter samples were removed from the viscometer at specific time points during the cell adhesion experiment and fixed in 100 μL of cold 2% glutaraldehyde for subsequent flow cytometry analysis using a FACSCalibur flow cytometer (Becton Dickinson). For this analysis, the neutrophil population in fixed samples was identified on the basis of its characteristic forward vs side scatter profile, and the number of singlets and aggregates of various sizes were resolved using the autofluorescence imparted by glutaraldehyde fixation (25). The extent of homotypic adhesion (fraction aggregation) was determined by monitoring the depletion of single neutrophils using the following equation: fraction aggregation = $1 - S/(S + 2D + 3T + 4Q + 5P+)$; where S is the number of singlets, D denotes doublets, T is for triplets, Q for quadruplets, and $P+$ denotes pentuplets and larger aggregates.

A previously developed mathematical model (26, 27) was applied to further analyze the rates of cell adhesion in terms of “adhesion efficiencies”. Adhesion efficiency is defined as the fraction of cell–cell collisions that results in aggregate formation. It is by definition always ≤ 1 . This parameter was computed for each of the individual runs by fitting the flow cytometric data above for the first 40 s of the aggregation experiment. These efficiency data for each treatment were normalized with respect to a positive control performed with the same donor blood. In this control, neutrophils were stimulated and sheared in the absence of any antagonist. On the basis of this normalized data, we determined the IC_{50} values, the concentration of the inhibitor that reduced neutrophil adhesion efficiency by 50%, by interpolation.

L- and P-Selectin Chimera Static Binding. Human L- (4 $\mu\text{g}/\text{mL}$) or P-selectin (3 $\mu\text{g}/\text{mL}$) IgG chimera (GlycoTech, Gaithersburg, MD) were incubated with saturating amounts of goat-anti-human $\text{F}(\text{ab}')_2$ FITC-conjugated secondary antibody (6 $\mu\text{g}/\text{mL}$) in HEPES buffer containing 1.5 mM Ca^{2+} and 1% goat serum (Jackson ImmunoResearch) at 37 °C for 10 min. Isolated neutrophils were then added at a final concentration of 0.5×10^6 cells/mL. The extent of chimera binding to their ligands on neutrophils was determined using flow cytometry. In negative control runs, FITC-conjugated secondary antibody alone, in the absence of selectin chimera, bound human neutrophils at least 1 order of magnitude lower than the positive controls with selectin chimera present. L-/P-Selectin binding levels in this paper were computed by subtracting the values of negative controls from each sample reading. In runs that monitored the inhibitory efficacy of specific carbohydrates, the selectin chimera was incubated

with the antagonist and secondary antibody for 10 min at 37 °C prior to addition of neutrophils. In other runs that measured L-selectin IgG chimera dissociation from neutrophils, labeled L-selectin chimera (7 $\mu\text{g}/\text{mL}$) was allowed to bind to saturating levels on human neutrophils for 40 min. Cells were subsequently pelleted by centrifugation followed by resuspension in HEPES buffer that lacked soluble selectin. The time of resuspension was designated $t = 0$. L-Selectin dissociation from neutrophils was subsequently measured both in the presence and in the absence of 2 mM TBC1269. Here, TBC1269 was added to prevent selectin rebinding to neutrophils. In cases where the data are presented in normalized form, the geometric mean fluorescence intensity of a given sample is divided by the geometric mean fluorescence intensity of the positive control runs. On the basis of this normalized data, the concentration of inhibitor that blocked 50% of selectin chimera binding to neutrophils was designated to be the IC_{50} .

Surface Plasmon Resonance. All surface plasmon resonance experiments were performed using a Biacore 3000 instrument (Biacore Inc., Piscataway, NJ) at 25 °C. The running buffer was phosphate buffered saline (PBS; 10 mM phosphate, 150 mM NaCl, pH 7.0, 0.005% v/v surfactant P-20) that was supplemented with either 1 mM calcium or 3 mM EDTA (in the absence of calcium). For all experiments, a polyclonal rabbit anti-mouse Fc specific antibody (Biacore Inc., Piscataway, NJ) was first immobilized onto research grade CM5 sensor chips via amine coupling using the manufacturer’s protocol (Biacore). In typical experiments, a 3-fold dilution of P-selectin-IgG from insect cell-culture supernatant was injected at 5 $\mu\text{L}/\text{min}$ for 8 min over a single flow cell, designated the active flow cell. Following P-selectin-IgG coupling to substrate, the flowpath was changed to include a reference flow cell containing only immobilized rabbit anti-mouse antibody upstream of the active flow cell. The flow rate was increased to 50 $\mu\text{L}/\text{min}$. Then, four 1-min injections of 1 M NaCl were performed to remove nonspecifically bound supernatant components from the sensor chip surface. Running buffer was allowed to flow through the flow cells for 20 min before analyte (e.g. TBC1269) injections were performed. Analyte was injected using the KINJECT command with a 300 s dissociation time over the reference and active flow cells at a fixed concentration in running buffer for 1 min. Following analyte injection, two 1-min 20 mM HCl injections were performed to regenerate the surface back to unbound rabbit anti-mouse Fc (i.e. all bound P-selectin and analyte were removed). The cycle was then repeated beginning with the loading of fresh P-selectin-IgG. An example of the typical cycle is shown in Figure 4A. Binding of carbohydrate to selectin-bearing substrate was measured in response units (1 RU = 1 pg of protein/ mm^2). Other variations of this experiment including controls are elaborated upon in Results.

For equilibrium studies, data were collected simultaneously from the active and reference flow cells at 1 point s^{-1} . The response observed on the reference cell was first subtracted from that of the active cell to yield reference subtracted data. Reference subtracted data from a blank buffer injection were then further subtracted from each of the analyte treatments to yield double-referenced subtracted sensorgrams. The binding response at equilibrium (R_{eq}) for each analyte injection was extracted from this sensorgram by averaging

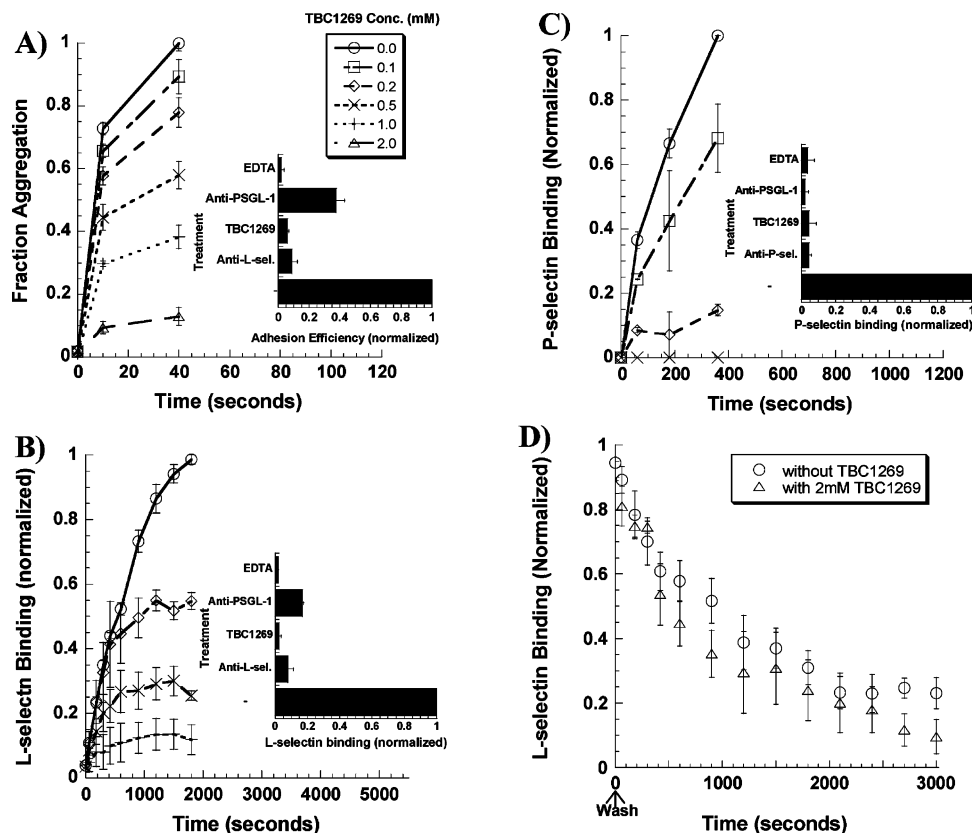


FIGURE 2: Static and shear assays. In panels A–C the ability of various doses of TBC1269 (up to 2.0 mM) to block selectin binding function was assayed. The inset to each panel presents control experiments that confirm the specificity of the binding interaction studied. (A) Cone-plate viscometer experiments that measure L-selectin mediated homotypic neutrophil aggregation under fluid flow. (B) L-Selectin chimera binding to isolated human neutrophils under static conditions measured using flow cytometer. (C) P-Selectin chimera binding to neutrophils measured using flow cytometer. (D) L-Selectin dissociation from neutrophils. Here, L-selectin chimera was allowed to bind to saturating levels on human neutrophils for 40 min. Cells were subsequently washed and resuspended either in the presence or in the absence of 2 mM TBC1269 and the dissociation of selectin from neutrophils was measured using flow cytometry. The time of resuspension was designated $t = 0$. Data are mean \pm SEM for 2–5 experiments.

the binding level over a 5 s interval 5 to 10 s prior to the end of the injection. Affinity constants were determined from a nonlinear curve fit, using the steady state affinity model provided in BIAevaluation (Version 4.1). Scatchard plots were made for alternative visualization of the data.

In runs performed to quantify the dissociation rate constants (k_{off}) of the molecular interaction, 1.16 mM TBC1269 was injected into the flow cell and its elution from the sensor surface was quantified by comparing the changes in the response of the active and reference flow cells following the end of the analyte injection. Data were collected at 5 points s^{-1} (0.2 s time resolution) as this is the highest data acquisition rate for two cells in series. Since the reference and active flow cells are in series, there is a slight delay in the precise time when elution begins in each of the flow cells. The magnitude of this time delay depends on the dead volume between the flow cells and the buffer flow rate. Additionally, there is an uncertainty as to when the elution begins in each flow cell. The reason for this uncertainty is that while the response of each cell is observed to drop abruptly from one time point when signal is at steady state to a lower value at the next data point after elution begins, the precise instant when the drop begins in this 0.2 s interval is not known. In order to compensate for this uncertainty, the data for the active and reference flow cells were shifted such that the bulk refractive index decrease in the reference cell was approximately first-order, and the

signal drop in the active cell was either equal to or greater than that in the reference cell. On the basis of this rationale, the time delay used for our runs was 0.28 s. As elaborated in Results, while the precise measure of k_{off} can vary slightly depending on the time delay employed, our experiments do indicate differences from the nature of TBC1269 elution between the active and the reference cell.

Carbohydrate Size Exclusion Chromatography. TBC1269 was perfused through a 50 cm Biogel P-2 size exclusion column (MW cutoff of 1800 Da; Biorad Laboratories, Hercules, CA) that was equilibrated with PBS. Fractions (~ 0.26 mL) were collected until PBS equal to 4 times the void volume had passed through the bed. Total carbohydrate concentration in each fraction was determined using an anthrone colorimetric assay. For this assay, each sample was mixed on ice with 0.75% (w/v) anthrone solution made in 84% (v/v) sulfuric acid. The samples were immediately heated to 100 $^{\circ}\text{C}$ for 10 min, cooled rapidly on ice, and moved to -20 $^{\circ}\text{C}$ for 5 min. The absorbance of each sample was then measured at 590 nm using a spectrophotometer. A calibration curve was constructed with known concentrations of TBC1269 to quantify the amount of the compound appearing within the void volume and in subsequent fractions. The above runs were performed both in the presence and in the absence of calcium.

Statistical Analysis. Error bars represent standard error mean (SEM) in all cases. Student's t -test was used to test

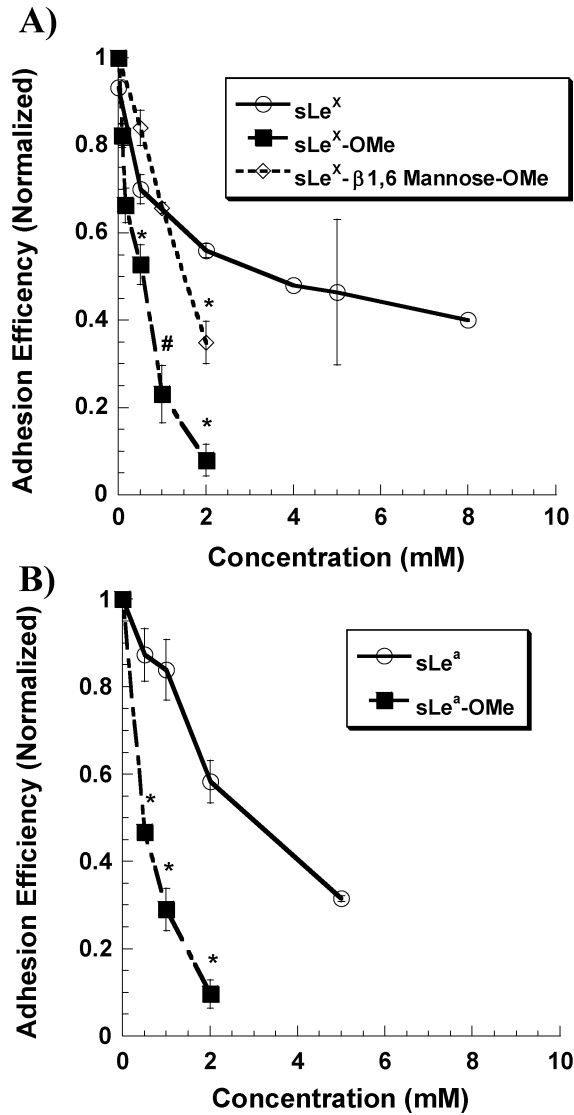


FIGURE 3: Effect of aglycon group on blocking efficacy of oligosaccharides in shear assays. Neutrophils were incubated with varying concentrations of sLe^x, sLe^x-β1,6Man-OMe and sLe^x-OMe (panel A), and sLe^a and sLe^a-OMe (panel B) prior to fMLP stimulation and application of fluid shear. Fraction aggregation was quantified at each sampling point by flow cytometric analysis of glutaraldehyde-fixed samples. Adhesion efficiency was determined and normalized with respect to runs without any added inhibitors. Data are mean ± SEM for 2–5 experiments. (*) *p* < 0.05 with respect to sLe^x or sLe^a at same dose. (#) *p* < 0.05 with respect to sLe^x-β1,6Mannose-OMe at same dose.

for statistical significance when two treatments were compared. ANOVA analysis and Student–Newman–Keuls post-tests were performed for multiple comparisons. *p* < 0.05 was considered significant.

RESULTS

Specificity of Selectin–Ligand Interaction in Shear and Static Experiments. We investigated the ability of the oligosaccharides listed in Table 1 both to block neutrophil aggregation under shear and to inhibit L- and P-selectin IgG binding to neutrophils under static conditions (Figure 2). In the homotypic aggregation assay (Figure 2A), we observed a dose dependent inhibition of aggregation upon addition of varying amounts of carbohydrates. Data for TBC1269 are presented in this figure. Various controls were performed to

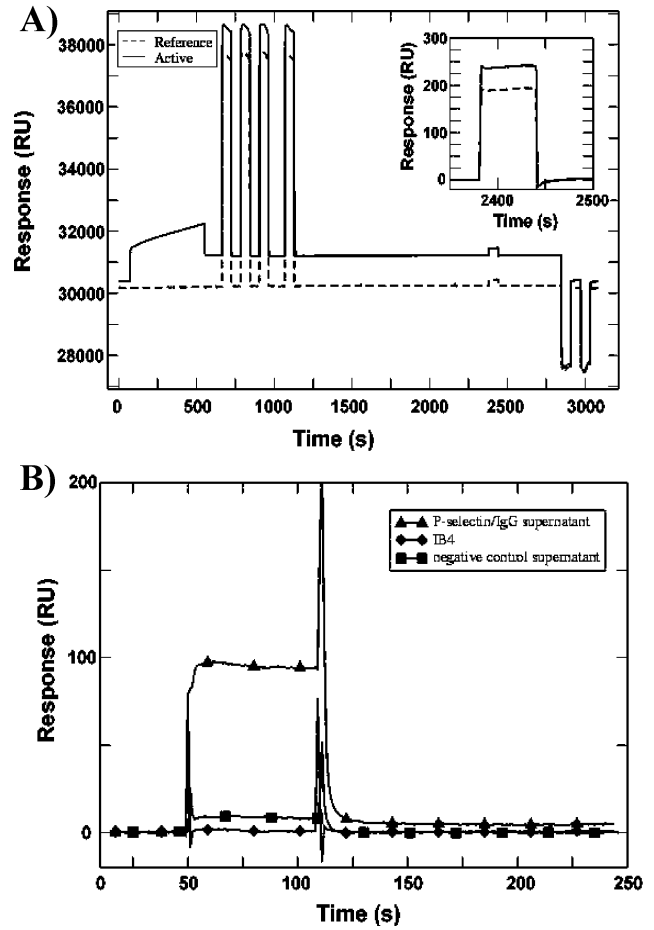


FIGURE 4: Surface plasmon resonance for selectin–ligand interactions. (A) Representative experiment cycle where P-selectin-IgG was immobilized in the active flow cell (solid line) by injecting diluted protein from cell culture supernatant at 5 μL/min for 8 min over a CM5 sensor chip bearing covalently linked rabbit anti-mouse Fc specific antibody. The reference flow cell (dashed line) was upstream of the active flow cell. This cell was identical to the active cell except for the absence of immobilized selectin. Selectin immobilization was followed by four 1 min injections of 1 M NaCl at 50 μL/min, a 20 min flow of running buffer, and finally a 1 min injection of analyte (145 μM TBC1269). Two 1 min 20 mM HCl injections were performed to regenerate the surface at the end of the cycle. The inset presents an expanded view of the net response in the active cell (solid line) and the reference flow cell (dashed line) to TBC1269 injection. (B) In negative control experiments, culture supernatant from mock-infected cells and isotype matched control antibody (clone IB4, mouse IgG2a) were made to flow over the sensor instead of P-selectin chimera in some runs during production of the active surface. TBC1269 did not bind these surfaces. Data are reference subtracted sensorgrams for TBC1269 at 1.16 mM.

establish the specificity of the interaction studied (inset to Figure 2A). As seen, cell adhesion was primarily L-selectin mediated since it could be blocked by an anti-L-selectin antibody DREG-56. It was Ca²⁺-dependent since EDTA abrogated it. Homotypic adhesion could also be partially blocked upon blocking PSGL-1 with mAb PL1, which is consistent with findings that neutrophils express L-selectin ligands that are distinct from PSGL-1 (28).

Similar to the shear runs, binding of both L- (Figure 2B) and P-selectin (Figure 2C) chimera to human neutrophils could be blocked by TBC1269 in a dose dependent manner. The specificity of both selectins binding to their ligands on neutrophils was confirmed (insets to Figure 2B and 2C).

Preincubation with an L-selectin blocking mAb DREG-56 for L-selectin chimera, or P-selectin blocking mAb G1 for P-selectin, completely blocked specific binding of chimeric molecules to neutrophils. Likewise, addition of EDTA abrogated selectin binding. Anti-PSGL-1 mAb, PL1, completely blocked P-selectin binding while it blocked ~80% of L-selectin chimera binding to neutrophils. Since TBC1269 blocked L-selectin mediated cell adhesion (Figure 2A) and L-selectin fusion protein binding (Figure 2B) over a similar dose range, our findings suggest that neutrophil homotypic adhesion rates exhibit a linear or first-order dependence on cell-surface selectin number.

The selectin chimera binding interaction described here is multivalent in nature as indicated by the slow binding rates, which approach equilibrium at ~10 min (Figure 2B,C), and slow dissociation kinetics, which proceeds on the order of minutes (Figure 2D). While some of the multivalency is due to the dimeric nature of the selectin fusion protein, there is also a major contribution of the secondary FITC-conjugated antibody used for flow cytometry detection, which cross-links the soluble selectin. This last statement is supported by experiments where P-selectin chimera was incubated with human neutrophils either in the presence or in the absence of unlabeled secondary antibody for 15 min at room temperature, prior to washing the cells, probing the bound selectin with a goat anti-mouse Alexa488-conjugated secondary Ab for 5 min and detection using flow cytometry (data not shown). In these experiments, we observed that dimeric selectin binding to neutrophils could only be detected when the unlabeled secondary antibody was added during the selectin incubation step. Thus, selectin cross-linking using secondary antibody is necessary for subsequent cytometry detection.

Chemical Composition of Aglycon Group Can Affect Blocking Efficacy. sLe^X is synthesized with various chemical groups at the anomeric position depending on the synthesis scheme utilized. We examined the degree to which the chemical entity at the anomeric position affects selectin-binding inhibition efficacy by performing homotypic neutrophil adhesion experiments in the presence of selected compounds. Here, we compared the blocking efficacy of sLe^X-OMe and sLe^X-β1,6Mannose-OMe with sLe^X (Figure 3A), and sLe^a-OMe with sLe^a (Figure 3B). These experiments were carried out with each molecule over a range of dosages using a protocol identical to that described in Figure 2A. The IC₅₀, which represents the reagent concentration that reduced cell adhesion efficiency by 50%, was determined. We observed that the IC₅₀ values for sLe^X and sLe^a were ~5- to 7-fold larger than their corresponding methyl glycosides. The inhibition efficacy of sLe^X-β1,6Mannose-OMe lay between that of sLe^X and sLe^X-OMe.

Comparison of Oligosaccharide Blocking Efficacy under Shear and Static Conditions. We quantified the ability of the panel of simple oligosaccharides and molecules containing the core-2 structure to block selectin mediated binding by quantifying their IC₅₀ in the three assays described in Figure 2: (i) L-selectin mediated homotypic neutrophil aggregation, (ii) L-selectin chimera binding assay, and (iii) P-selectin chimera binding assay (Table 1). Many of the compounds synthesized are unique since they are based on the capping groups of physiologically important glycans expressed on PSGL-1 and GlyCAM-1. We observed that

sLe^X-OMe, sLe^a-OMe, and the sLe^X analogue (TBC1269) were comparable in their ability to block L-selectin binding to human neutrophils and homotypic neutrophil aggregation. sLe^X and sLe^a also blocked P-selectin chimera binding to neutrophils with equal efficacy. Oligosaccharides based on the exact carbohydrate structures of capping groups of PSGL-1 (compound **1**) (**9**) and GlyCAM-1 (compound **2**) (**29**) were surprisingly poor inhibitors of L-selectin mediated binding and adhesion. They had affinities that were only ~30–150% higher than that of sLe^X. In studies with P-selectin chimera, glycans of PSGL-1 [**1**] and GlyCAM-1 [**2**] were poorer inhibitors of selectin binding than even sLe^X. The sulfated carbohydrate of GlyCAM-1 [**2**] was better at blocking L-selectin binding to neutrophils and neutrophil homotypic aggregation in comparison to soluble PSGL-1 oligosaccharide [**1**]. In contrast, the oligosaccharide based on PSGL-1 [**1**] rather than GlyCAM-1 [**2**] was marginally more effective at blocking P-selectin binding to neutrophils, though this difference was not statistically significant. Consistent with other published reports, sulfated oligosaccharides (compounds **5–7**) were superior inhibitors of L-selectin rather than P-selectin mediated binding. Of all the compounds tested, **3** was the best inhibitor tested, and it blocked both L- and P-selectin binding in the ~50 μM range. It was a 30–100-fold better inhibitor of selectin function than sLe^X.

The ability of various sulfated structures to inhibit L-selectin function was examined in detail since such carbohydrates have been shown to bind L-selectin. Here, we compared the capping group of GlyCAM-1 [**2**] with **5** to determine if sialic acid attached to the Galβ1–3GalNAc chain influences selectin binding. No statistically significant difference in blocking efficacy was observed. A comparison of compound **6** with **7** revealed that sulfation at the 6-position of GlcNAc enhanced inhibition of L-selectin mediated binding. Further, the L-selectin blocking function under static and shear conditions occurred over a similar dose range for all the oligosaccharides tested, except for the nonfucosylated molecule (compound **4**), which consistently exhibited weak blocking under static conditions and greater inhibition under fluid shear.

Overall, the blocking ability of most of the oligosaccharides designed based on the core-2 structure, especially **1** and **2**, was lower than we anticipated. The poor binding of oligosaccharides from PSGL-1 and GlyCAM-1 suggests that the protein portion of these molecules contributes substantially to ligand recognition, either by displaying multiple ligand epitopes or by directly stabilizing the interaction. A compound with no net charge (compound **3**) was identified that exhibited remarkable inhibition properties compared to the other molecules.

Binding Specificity in Biacore Experiments. P-Selectin-IgG was immobilized on the Biacore sensor surface at 810–1020 RU as detailed in Materials and Methods (Figure 4A). An expanded view of the nonspecific and specific response due to analyte injection (inset to Figure 4A) shows that the binding interaction reaches saturation rapidly and returns to the baseline within seconds of the end of the analyte injection.

Control experiments were performed to verify the specificity of the binding interactions (Figure 4B). Proteins from the P-selectin chimera cell culture supernatant were not

Table 1: Chemical Formulas, Common Names, and IC₅₀ Values for Synthetic Selectin Inhibitors^a

Structure	Common Name/Number	Homotypic Neutrophil IC ₅₀ (mM)	L-selectin Chimera IC ₅₀ (mM)	P-selectin Chimera IC ₅₀ (mM)	References
NeuAcα2-3Galβ1-4(Fucα1-3)GlcNAcβ1-OMe	sLe ^X -OMe	0.6 ± 0.06 ⁶	0.255 ± 0.013 ¹	2.2 ± 0.56	(48)
NeuAcα2-3Galβ1-4(Fucα1-3)GlcNAcβ1-OH	sLe ^X	5.0 ± 0.70	6.3 ± 0.50 ²	1.9 ± 0.50	(From Toronto Res. Chemicals)
NeuAcα2-3Galβ1-4(Fucα1-3)GlcNAcβ1-6Man-OMe	sLe ^X -β1,6O-Man-OMe	2.03 ± 0.12	1.05 ± 0.10	2.10 ± 0.23	(48)
NeuAcα2-3Galβ1-3(Fucα1-4)GlcNAcβ1-OMe	sLe ^a -OMe	0.8 ± 0.09 ⁶	1.23 ± 0.09 ³	No Data	
NeuAcα2-3Galβ1-3(Fucα1-4)GlcNAcβ1-OH	sLe ^a	2.5 ± 0.06 ⁸	3.80 ± 0.54	2.3 ± 0.20	
NeuAcα2-3Galβ1-4(Fucα1-3)GlcNAcβ1 NeuAcα2-3Galβ1-3GalNAcα1-OMe	Glycan of PSGL-1, 1	4.88 ± 0.86	4.2 ± 0.37 ⁴	2.7 ± 0.10	(49)
NeuAcα2-3Galβ1-4(Fucα1-3)(6SE)GlcNAcβ1 NeuAcα2-3Galβ1-3GalNAcα1-OMe	Glycan of GlyCAM-1, 2	3.07 ± 0.58	2.1 ± 0.13	3.5 ± 0.30 ¹¹	(49)
Galβ1-4(Fucα1-3)GlcNAcβ1 GalNAcβ1-3GalNAcα1-OMe	3	0.0625 ± 0.01	0.053 ± 0.003	0.055 ± 0.003	(50)
Galβ1-4(6SE)GlcNAc β1 NeuAcα2-3Galβ1-3GalNAcα1-OMe	4	3.2 ± 0.40	7.9 ± 0.90	4.5 ± 0.70 ¹⁰	
NeuAcα2-3Galβ1-4(Fucα1-3)(6SE)GlcNAc β1 Galβ1-3GalNAcα1-OMe	5	2.6 ± 0.40	2.1 ± 0.27	No Inhibition	
Galβ1-4(Fucα1-3)GlcNAc β1 (6-SE)Galβ1-3GalNAcα1-OMe	6	3.3 ± 0.70	3.1 ± 0.68	No Inhibition	(11)
Galβ1-4(Fucα1-3)(6-SE)GlcNAc β1 (6-SE)Galβ1-3GalNAcα1-OMe	7	1.9 ± 0.30 ⁷	2.5 ± 0.41	6.0 ± 1.00 ⁹	
1,6-bis[3-(3 carboxymethylphenyl)-4-(2-α-D-mannopyrano-syloxy)phenyl]hexane	TBC1269	0.5 ± 0.05 ⁶	0.4 ± 0.03 ⁵	0.27 ± 0.05 ⁹	(17, 18)

^a In Table 1, $p < 0.05$ for L-selectin static experiments with respect to (1) all treatments except sLe^a-OMe; (2) all other treatments; (3) all treatments except sLe^X-OMe, GlyCAM-1, **5**, **7**, and TBC1269; (4) all treatments except sLe^a and **6**; (5) all treatments except sLe^X-OMe and sLe^a-OMe. $p < 0.05$ for L-selectin shear experiments with respect to (6) all treatments except compound **7** (no difference between sLe^X-OMe, sLe^a-OMe and TBC1269); (7) **7** is different from **6**, PSGL-1, and sLe^X only; (8) all treatments except GlyCAM-1, **4**–**7**. $p < 0.05$ for P-selectin static experiments with respect to (9) all other treatments; (10) all treatments except GlyCAM-1; (11) all treatments except sLe^X-OMe, compound **4**, and PSGL-1.

observed to bind CM5 sensor chips in the absence of immobilized rabbit anti-mouse antibody (data not shown). TBC1269 did not bind to sensor chip surface bearing isotype control mAb (clone IB4). In these experiments, IB4 was immobilized at levels similar to immobilized P-selectin-IgG in the positive control. Supernatant from mock infected insect cells (without P-selectin-IgG) also exhibited very little binding to the rabbit anti-mouse Fc sensor surface. Subsequent injection of TBC1269 over these control surfaces resulted in a low response.

To confirm that the binding of the sLe^X analogue TBC1269 to P-selectin was specific, we quantified the ability of TBC1269 to inhibit the binding of P-selectin function blocking mAbs (G1 and humanized EP5C7) to immobilized P-selectin-IgG (Figure 5). Both antibodies block the interaction of P-selectin with human PSGL-1 even though they bind to different epitopes of P-selectin. While G1 binds the lectin domain of this protein, EP5C7 binds near the lectin-EGF junction (30). In our studies, following P-selectin-IgG

immobilization, the free remaining rabbit anti-mouse sites on the sensor chip were blocked by excess mouse anti-TSH mAb (Seradyn, Indianapolis, IN) for 8 min at 5 μL/min. After wash and equilibration, anti-P-selectin and control mAbs were made to flow over the sensor either in the presence or in the absence of 1.16 mM TBC1269. We observed that G1 was captured at 120 RU within 1 min in the absence of TBC1269 and at a reduced level of 50 RU in the presence of the sLe^X analogue (Figure 5A). Likewise, EP5C7 was captured at ~100 RU and 35 RU in the absence and presence of TBC1269, respectively (Figure 5B). As expected, the control anti-CD11a antibody TS1/22 (isotype matched to G1) did not bind to immobilized P-selectin (Figure 5C). These results demonstrate that surface plasmon resonance experiments can be utilized to investigate the specificity of TBC1269 binding to P-selectin, since it can prevent the binding of function blocking antibodies against various domains of this protein. Steric or allosteric mechanisms may contribute to this blocking.

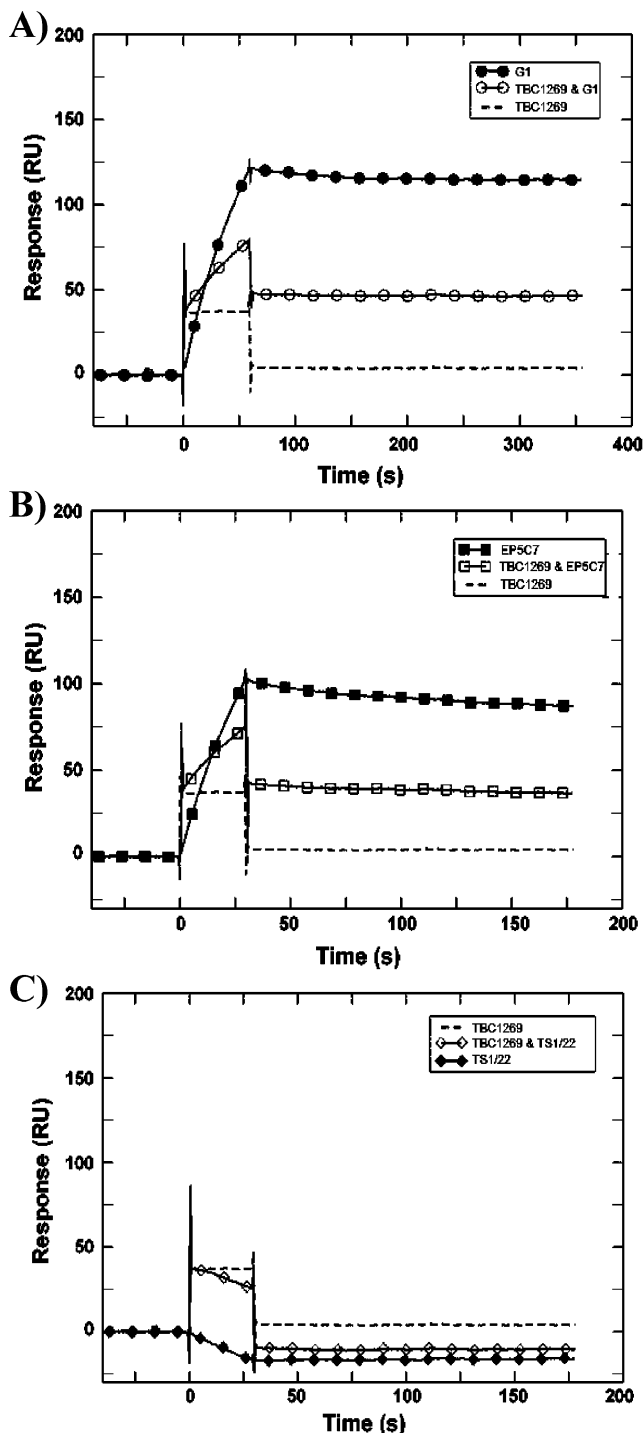


FIGURE 5: sLe^X analogue inhibits anti-P-selectin mAbs from binding immobilized P-selectin. Sensor substrates were prepared identically to Figure 4A with the exception that 200 µg/mL of a mouse anti-TSH mAb was made to flow over the active and reference cell for 8 min at 5 µL/min after P-selectin-IgG immobilization to block unoccupied rabbit anti-mouse sites. The wait time between the final wash and analyte injection was also reduced from 20 to 3 min. (A) 10 µg/mL P-selectin blocking mAb clone G1 that binds the lectin domain, (B) 20 µg/mL anti-P-selectin blocking antibody clone EP5C7 that binds the junction region between the lectin and EGF domains, or (C) 10 µg/mL isotype-matched control mouse mAb (anti-CD11a clone TS1/22) were made to flow over the sensor chips either with or without 1.16 mM TBC1269. TBC1269 chipped with both the P-selectin blocking antibodies. Data are reference subtracted sensorgrams.

Affinity and Kinetic Analysis of Selectin–Carbohydrate Interactions. Representative sensorgrams for experiments

performed over a range of TBC1269 concentrations are presented in Figure 6A,B. The observed maximum binding levels of TBC1269 to P-selectin-IgG was ~9 times higher than that theoretically expected on the basis of 1:1 stoichiometric binding, assuming that the refractive index increments ($\partial n/\partial C$) of the analyte and ligand are equal, and the ligand activity is 100%. When these assumptions are made, the stoichiometry of the interaction is calculated by $S = (R_{\max}/R_L)(MW_L/MW_A)$ where S is the number of analyte molecules capable of binding per immobilized ligand molecule, R_L is the amount of immobilized ligand (~1000 RU typically), R_{\max} is the response upon saturation of the ligand binding sites (160 in Figure 6A), and MW_L and MW_A are the molecular weight of the immobilized ligand (50 000 Da) and analyte (862.94 Da). This observation suggests that TBC1269, under our experimental conditions, may agglomerate to form a complex with itself.

To determine if TBC1269 forms aggregates, we perfused this reagent through a Biogel P-2 size exclusion column (MW cutoff of 1800 Da) under conditions identical to those used in the Biacore experiments, and assayed the eluate using the anthrone reaction. Both in the presence and in the absence of calcium, ~90% of the small molecule eluted with the column void volume, suggesting that the compound was aggregated. Because this molecule forms multimers, we use the term “apparent” K_D , instead of simply K_D , to describe the affinity data.

The equilibrium binding levels were extracted from sensorgrams in Figure 6A,B and plotted as a function of sLe^X analogue concentration (Figure 6C,D). These plots were fit to the steady state affinity model to determine the molecule’s affinity. Apparent K_D values in the presence and absence of Ca^{2+} were 111.4 (± 15.4) µM and 94.6 (± 4.5) µM, respectively, for four independent experiments. Even though the affinities calculated were not significantly different, the binding responses at equivalent TBC1269 concentrations were consistently higher (~25%) when Ca^{2+} was present. This resulted in statistically higher R_{\max} values for the Ca^{2+} data sets (Figure 6B, inset). The findings suggest that there may be a change either in the binding mechanism (i.e. number of binding sites available on immobilized ligand) or in the value of the stoichiometry parameter, S (i.e. the size of the TBC1269 complex), upon addition of calcium.

We attempted to measure the selectin–carbohydrate off rates (k_{off}) by following the elution of TBC1269 from the immobilized P-selectin substrate. We observed that the response of the active cell decayed at a slower rate than that of the reference cell (Figure 7). The off rate estimated for the active cell based on an exponential decay curve fit (method suggested in ref 31) was ~5 s⁻¹. This off rate includes the effect of two features: the removal of soluble, unbound TBC1269 from close to the substrate, and the dissociation of TBC1269 from immobilized P-selectin. Exponential curve fits of TBC1269 dissociation from immobilized P-selectin after reference subtraction were also performed (data not shown), and these yielded k_{off} in the range of 1–3 s⁻¹. The precise k_{off} estimated in these calculations depended on the value of the time-delay correction employed (see Materials and Methods). Since the elution of TBC1269 from the sensor surface is rapid, because this molecule forms multimers in solution, and since our calculations approach the detection limit of the Biacore

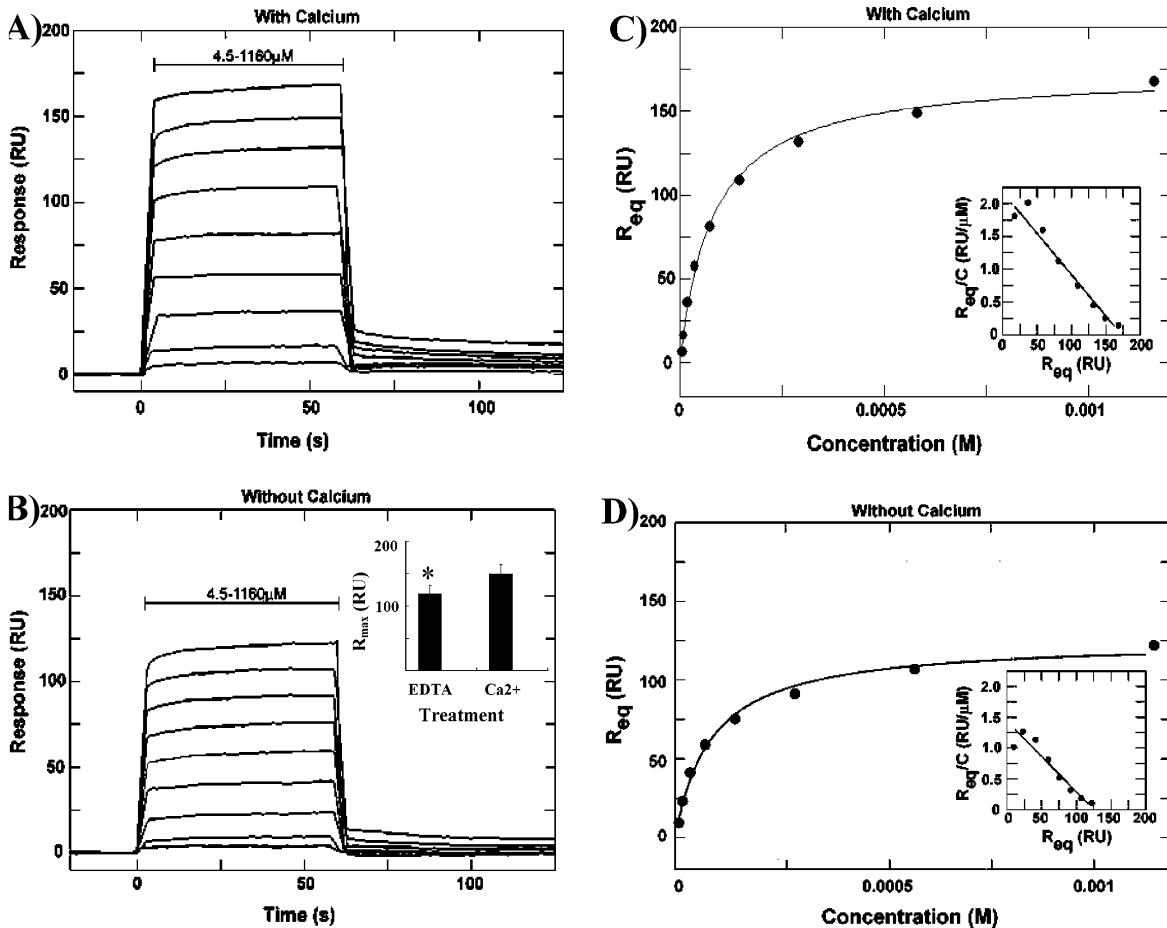


FIGURE 6: Affinity of sLe^X analogue binding to P-selectin. Representative sensorgrams of TBC1269 binding to immobilized P-selectin in the presence of (A) 1 mM Ca²⁺ and (B) 3 mM EDTA (no Ca²⁺). Here, sLe^X analogue concentration was varied from 1.16 mM down to 0.0045 mM by serially diluting analyte by a factor of 2. A dose-dependent binding response is noted. Binding affinity fit using the steady state affinity model in the presence of (C) 1 mM Ca²⁺ or (D) 3 mM EDTA (no Ca²⁺). Scatchard plot is also shown in the inset. The calculated affinities (K_D) of TBC1269 binding to P-selectin in the presence and absence of Ca²⁺ were not significantly different. However, the maximum binding response (R_{eq} in runs with 1.16 mM TBC1269) was greater in the presence of Ca²⁺ (inset to panel B). (*) $p < 0.05$ with respect to Ca²⁺ run.

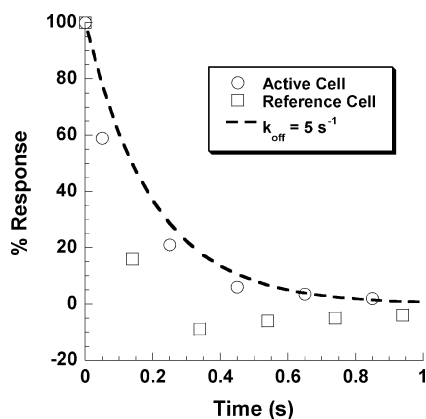


FIGURE 7: Kinetics of sLe^X analogue dissociation from P-selectin. TBC1269 (1.16 mM) was injected for 8 min at 50 μ L/min over the reference (no P-selectin) and active (\sim 600 RU of immobilized P-selectin) flow cells that were arranged in series in a Biacore3000 instrument. TBC1269 dissociation was monitored following elution at the same flow rate. Data (discrete points) acquired at a rate of 5 points s⁻¹ were offset by a time delay as described in Materials and Methods, and then normalized with respect to the maximum binding signal for the reference (199 RU) and active (234 RU) flow cells, respectively. Results are plotted as % response vs time for the reference (squares) and active (circles) cells. Dashed line represents exponential decay curve fit with a k_{off} value of 5 s⁻¹.

instrument, we conservatively conclude that the k_{off} for TBC1269 P-selectin interaction is ≥ 3 s⁻¹. Thus, k_{on} is $\geq 27\,000$ M⁻¹ s⁻¹. Overall, the results suggest a very rapid binding on and off rate for selectin–carbohydrate interaction, along with both calcium-dependent and -independent binding mechanisms.

DISCUSSION

Adhesion and Binding Assays. We applied flow cytometry to study selectin–ligand binding under static conditions and cone-plate viscometry to assay inhibitor efficacy under hydrodynamic shear. In general, we observed that the dosages of the small molecule required for blocking cell adhesion under hydrodynamic shear and for blocking L-selectin chimera binding under static conditions were comparable. The IC₅₀ for blocking was also comparable when TBC1269 was used to inhibit P-selectin fusion protein binding to isolated neutrophils in the cytometry studies, versus the ability of this carbohydrate to inhibit P-selectin binding to recombinant, immobilized PSGL-1 (19.ek.Fc, ref 32) in ELISA based experiments (data not shown). While the IC₅₀ in the former experiments was measured to be 0.27 mM, it was 0.55 mM in the ELISA runs. Overall, these observations

suggest a first-order/linear dependence of cell adhesion on selectin number.

Our rationale for choosing flow cytometry based methods over the more conventional ELISA-based competitive inhibition assay (11) or flow chamber experiments (33) is 4-fold. First, the sample volume required for each experiment is relatively small ($\sim 60 \mu\text{L}$), yet we are able to study the function of the synthetic molecule under both static and fluid flow conditions. This allowed us to work with selectin–ligand analogues that were available in scarce quantities. Second, data obtained using these techniques are very reproducible since we are examining the average of several thousand binding events or collisions for static or shear experiments, respectively. Collisions observed in flow chamber studies are limited to the field of view of the microscope. Third, since selectin–oligosaccharide binding takes place with rapid on and off rates, our protocol does not involve wash steps that may complicate data interpretation. Finally, while the valency of selectins can regulate the specificity of protein–carbohydrate recognition in ELISA-based studies (23), the use of human neutrophils in our studies allows us to screen selectin inhibitors using the naturally occurring valency of selectins and their ligands. While the flow cytometry assays allowed us to compare the relative binding efficacies of our reagents in small volumes, these measurements were a result of multivalent selectin interaction with their carbohydrate ligand. Therefore, to complement this measurement strategy, we employed surface plasmon resonance to assay single molecule binding kinetics.

Oligosaccharide Blocking Efficacy. Studies investigating an oligosaccharide's blocking ability typically utilize $s\text{Le}^x$ as the standard for quantifying inhibition efficacy. This standard is important for a relative comparison of results between different research groups since the panel of molecules tested often differ, as does the experimental strategy used to quantify IC_{50} (5). In the current manuscript, we demonstrate that the functional group at the anomeric position can dramatically affect $s\text{Le}^x$ binding function. Methyl glycosides of $s\text{Le}^x$ and $s\text{Le}^a$ were observed to be superior inhibitors of selectin binding compared to $s\text{Le}^x$ and $s\text{Le}^a$. This observation is supported by other reports which demonstrate that the addition of a hydrophobic unit, such as an alkyl or lipid chain, can enhance selectin antagonist function (5, 16, 34). Leppanen et al. (35) also show that while the PSGL-1 sulfopeptide with $s\text{Le}^x$ at the 6-position of GalNAc can bind P-selectin, an isomer where $s\text{Le}^x$ is located on the extended core-1 chain is not active. Our observed difference in blocking ability may be due to several reasons including, but not limited to, the ability of the more hydrophobic methyl group to act as an "anchor" stabilizing the otherwise transiently bound molecule, alterations in the molecular solubility, changes in the 3-dimensional conformation of the oligosaccharide in solution, or changes in the nature of its complexation with L-selectin.

Our inhibition studies focus on L- and P-selectin since these selectins primarily recognize core-2 based glycans while E-selectin has been shown to bind N-glycans also. Our observation that the glycan of PSGL-1 [1] blocks L- and P-selectin binding function is not surprising given that this is its natural ligand. The carbohydrate of GlyCAM-1 [2] is also a prominent ligand for L-selectin. Finally, our observation that GlyCAM-1 blocks P-selectin function is reasonable

given observations that activated platelets bind PNAd/MECA-79 (peripheral node addressin) epitopes on high endothelial venules (HEVs) (36). GlyCAM-1 is a component of PNAd. In studies aimed to address the relative importance of $\alpha(2,3)$ sialic acid linkage to the Gal β 1,4GlcNAc versus the Gal β 1,3GalNAc arms of the core-2 moiety in contributing to selectin recognition, we did not observe any significant difference in the blocking function of 2 versus 5 for L-selectin. Finally, sulfated glycans were observed to be more effective at blocking L-selectin binding function compared to P-selectin.

While the specificity of the interactions we studied is consistent with data in the literature, we observed that 1 and 2 inhibited selectin binding in the 2–5 mM range. This corresponds to binding affinities that were on the same order of magnitude as that of $s\text{Le}^x$. In comparison, we have previously designed core-2 based structures that bind selectins with severalfold greater affinities than $s\text{Le}^x$ (22). Recent studies also report that $s\text{Le}^x$ -type carbohydrates with a core-2 structure linked to two structurally similar N-terminal PSGL-1 glycosulfopeptides bind selectins with high affinities ($K_D \sim 0.35$ to $0.78 \mu\text{M}$) (35). Also, GlyCAM-1 was shown to bind to L-selectin with a dissociation constant of $108 \mu\text{M}$ (31). The differences in our observations and those of others (32) could be due to the absence of tyrosine sulfation and/or the peptide chain in our synthetic molecule. Besides the importance of the peptide chain in ligand recognition, our studies also indicate that the net charge of the soluble molecules may be an important parameter regulating selectin recognition. This property controls the partitioning of the small molecules between its free state in solution and its bound state with ligand.

Among the molecules we tested, we observed that compound 3 inhibited L- and P-selectin function, in the $50 \mu\text{M}$ range, at ~ 30 – 100 -fold lower doses than $s\text{Le}^x$. 3 is unique since the carbohydrate has no negative charge (no sialic acid or sulfate group). The exact structural features that contribute to the enhanced binding of this molecule to L- and P-selectin, and the possibility that the attachment of $s\text{Le}^x$ to the 6-position of GalNAc α will further enhance inhibition function, are currently being studied in our laboratory.

Affinity and Kinetics for $s\text{Le}^x$ Analogue Binding to Selectin. We quantified the affinity and kinetics of $s\text{Le}^x$ analogue, TBC1269, binding to P-selectin using surface plasmon resonance. TBC1269 formed multimers in these experiments as suggested by both surface plasmon resonance and size exclusion chromatography measurement. It was, however, difficult to estimate the exact size of these multimers and their distribution from surface plasmon resonance runs since the refractive index increment ($\partial n/\partial C$) of the small molecule is unknown, and it may be significantly different from that of proteins (37). While the dimeric nature of TBC1269 and the $(\text{CH}_2)_4$ alkyl chain that space the functional units (Figure 1) have been shown to contribute to selectin recognition (17), our studies suggest that carbohydrate multimerization may also contribute to the measured K_D . Multimeric presentation of inhibitors has been shown to increase molecular inhibition ability (5, 38) by promoting molecular rebinding effects. While the exact structural features contributing to multimerization are yet undetermined, we note that specific interaction between Le^x and Le^x determinants has been suggested

in the literature and this feature may contribute to carbohydrate aggregation (39). Also, another recent report has shown that some small molecules designed to target specific enzymes can form aggregates when applied at μM concentrations, and such aggregation can result in promiscuous inhibition of unrelated enzyme activities (40). Small-molecule multimerization is typically not accounted for in studies that assay selectin-inhibitor function. We now suggest that this may be an important feature contributing to the measured IC_{50} values reported in published literature.

TBC1269 was shown to retard, with nearly equal efficacy, the ability of two function-blocking antibodies to bind P-selectin. While one of the mAbs is directed against the lectin domain (clone G1) (41, 42), the second recognizes the lectin-EGF junction region (clone EP5C7) (30). One possible explanation is that TBC1269 sterically inhibits both mAbs from binding. Another possibility is that while TBC1269 sterically inhibits G1 binding, it may allosterically alter the conformation of the EP5C7 binding site and prevent this antibody from binding the selectin. The later function would suggest that subtle conformation changes in the lectin domain may propagate to other domains within the protein. Indeed, various studies have suggested that the EGF domain can allosterically modulate selectin binding function by altering selectin ligand binding specificity (43, 44) or enhancing selectin ligand recognition (45). Also, Sommers et al. have shown that PSGL-1 binding to P-selectin may cause a structural change at the hinge region between the lectin-EGF domains (32). In the same study, sLe^x was shown not to cause a structural change in this region. The authors argue that this may be due to steric contacts in the preformed P-selectin crystals (32).

Both calcium-dependent and -independent mechanisms may contribute to sLe^x analogue binding to P-selectin. In support of the requirement of Ca^{2+} , we observed that the R_{max} value was significantly higher in the presence of Ca^{2+} . However, at the same time, the K_{D} of TBC1269 binding to P-selectin was comparable both in the presence and in the absence of Ca^{2+} . Although calcium is absolutely required for L- and P-selectin binding to their ligands on neutrophils, it does not appear to be necessary for TBC1269 recognition of P-selectin. Analogous results have been reported by Koenig et al., who show that while P-selectin can bind heparin (tetradecasaccharides) in a calcium-independent manner, its recognition of L-selectin is calcium-dependent (21). Despite differences in the binding mechanism, this heparin molecule effectively inhibits L- and P-selectin adhesion function. Based on this, it will be interesting to investigate in the future if L-selectin recognition of TBC1269, unlike P-selectin, is purely calcium dependent.

Like previous studies of selectin–ligand binding (29, 31, 46, 47), TBC1269 binding to P-selectin displayed rapid kinetics with saturation/equilibrium binding being reached within seconds. Previously (46), it has been noted that the affinity of P-selectin PSGL-1 interaction is strong ($K_{\text{D}} = 0.32 \mu\text{M}$) and the off rate (1.4 s^{-1}) is lower in comparison with rat L-selectin binding to mouse GlyCAM-1 ($K_{\text{D}} = 108 \mu\text{M}$ and $k_{\text{off}} > 10 \text{ s}^{-1}$) (31) and mouse E-selectin ESL-1 interaction ($K_{\text{D}} = 62 \mu\text{M}$ and $k_{\text{off}} = 4.6 \text{ s}^{-1}$) (47). The binding affinities of E-selectin binding to ESL-1 and L-selectin recognition of GlyCAM-1 were comparable. Our current measurements show that the apparent K_{D} for TBC1269

P-selectin binding ($K_{\text{D}} = 111.4 \pm 15.4 \mu\text{M}$ with Ca^{2+} and $94.6 \pm 4.5 \mu\text{M}$ in the absence of Ca^{2+}) is comparable to that of L-selectin GlyCAM-1 binding, and it is substantially lower than the affinity of P-selectin-PSGL-1 binding. Our estimated k_{off} is $> 3 \text{ s}^{-1}$. We can expect that the tetrasaccharide sLe^x binding to selectin will also display similar rapid off rates.

Studies using flow cytometry and surface plasmon resonance can be used to predict the binding affinities of selectins for sLe^x and other scarce core-2 based synthetic compounds. In this context, the IC_{50} of TBC1269 inhibition of P-selectin binding in the static assays was 0.27 mM, while the apparent K_{D} for small-molecule selectin interaction using surface plasmon resonance was 2.5-fold lower at 111.4 μM . Based on this, we expect that other molecules listed in Table 1 would also have binding affinities measured using surface plasmon resonance that are 2.5-fold lower than the IC_{50} 's noted in this table. Thus, we expect that the K_{D} for L-selectin binding to the carbohydrate portion of GlyCAM-1 is ~ 0.84 – 1.23 mM . Since this value is 10-fold higher than the measured K_{D} for L-selectin binding to the GlyCAM-1 glycoprotein (0.108 mM), we suggest that either the protein core of GlyCAM-1 or the presentation of carbohydrates in clusters on this glycoprotein may contribute to L-selectin recognition.

Overall, our investigation reveals that oligosaccharides designed on the basis of the naturally occurring glycans of PSGL-1 and GlyCAM-1 were not potent selectin inhibitors. Compound 3, a novel molecule, was identified which blocks selectin binding under static and shear conditions at 30–100-fold lower doses than sLe^x. The mechanism of action of this molecule is currently being investigated. Finally, we provide the first direct measurement of the affinity and kinetic interactions of selectin interaction with a carbohydrate using surface plasmon resonance. These measurements demonstrate that an analogue of sLe^x exhibits low affinity ($K_{\text{D}} \sim 111.4 \mu\text{M}$) and rapid binding kinetics ($k_{\text{off}} > 3 \text{ s}^{-1}$ and $k_{\text{on}} > 27\,000 \text{ M}^{-1} \text{ s}^{-1}$). The studies emphasize the role of molecular hydrophobicity and protein core in regulating binding rates in vitro and in vivo.

ACKNOWLEDGMENT

We thank Zhihua Xiao for insect cell culture and E. V. Chandrasekaran for help with the Biogel P-2 assay.

REFERENCES

1. Neelamegham, S. (2004) Transport Features, Reaction Kinetics and Receptor Biomechanics Controlling Selectin and Integrin Mediated Cell Adhesion, *Cell Commun. Adhes.* 11, 35–50.
2. Ley, K., and Kansas, G. S. (2004) Selectins in T-cell recruitment to non-lymphoid tissues and sites of inflammation, *Nat. Rev. Immunol.* 4, 325–335.
3. Vestweber, D., and Blanks, J. E. (1999) Mechanisms that regulate the function of the selectins and their ligands, *Physiol. Rev.* 79, 181–213.
4. Lowe, J. B. (2003) Glycan-dependent leukocyte adhesion and recruitment in inflammation, *Curr. Opin. Cell Biol.* 15, 531–538.
5. Simanek, E. E., McGarvey, G. J., Jablonowski, J. A., and Wong, C.-H. (1998) Selectin-carbohydrate interactions: from natural ligands to designer mimics, *Chem. Rev.* 98, 833.
6. Snapp, K. R., Heitzig, C. E., Ellies, L. G., Marth, J. D., and Kansas, G. S. (2001) Differential requirements for the O-linked branching enzyme core 2 beta1-6-N-glucosaminyltransferase in biosynthesis of ligands for E-selectin and P-selectin, *Blood* 97, 3806–3811.

7. Sperandio, M., Thatte, A., Foy, D., Ellies, L. G., Marth, J. D., and Ley, K. (2001) Severe impairment of leukocyte rolling in venules of core 2 glucosaminyltransferase-deficient mice, *Blood* 97, 3812–3819.
8. Ellies, L. G., Tsuboi, S., Petryniak, B., Lowe, J. B., Fukuda, M., and Marth, J. D. (1998) Core 2 oligosaccharide biosynthesis distinguishes between selectin ligands essential for leukocyte homing and inflammation, *Immunity* 9, 881–890.
9. Wilkins, P. P., McEver, R. P., and Cummings, R. D. (1996) Structures of the O-glycans on P-selectin glycoprotein ligand-1 from HL-60 cells, *J. Biol. Chem.* 271, 18732–18742.
10. Leppanen, A., Yago, T., Otto, V. I., McEver, R. P., and Cummings, R. D. (2003) Model glycosulfopeptides from P-selectin glycoprotein ligand-1 require tyrosine sulfation and a core 2-branched O-glycan to bind to L-selectin, *J. Biol. Chem.* 278, 26391–26400.
11. Koenig, A., Jain, R., Vig, R., Norgard-Sumnicht, K. E., Matta, K. L., and Varki, A. (1997) Selectin inhibition: synthesis and evaluation of novel sialylated, sulfated and fucosylated oligosaccharides, including the major capping group of GlyCAM-1, *Glycobiology* 7, 79–93.
12. Berg, E. L., Magnani, J., Warnock, R. A., Robinson, M. K., and Butcher, E. C. (1992) Comparison of L-selectin and E-selectin ligand specificities: the L-selectin can bind the E-selectin ligands sialyl Le(x) and sialyl Le(a), *Biochem. Biophys. Res. Commun.* 184, 1048–1055.
13. Hiraoka, N., Kawashima, H., Petryniak, B., Nakayama, J., Mitoma, J., Marth, J. D., Lowe, J. B., and Fukuda, M. (2004) Core 2 branching beta1,6-N-acetylglucosaminyltransferase and high endothelial venule-restricted sulfotransferase collaboratively control lymphocyte homing, *J. Biol. Chem.* 279, 3058–3067.
14. Buerke, M., Weyrich, A. S., Zheng, Z., Gaeta, F. C., Forrest, M. J., and Lefer, A. M. (1994) Sialyl Lewisx-containing oligosaccharide attenuates myocardial reperfusion injury in cats, *J. Clin. Invest.* 93, 1140–1148.
15. Ohnishi, M., Imanishi, N., and Tojo, S. J. (1999) Protective effect of anti-P-selectin monoclonal antibody in lipopolysaccharide-induced lung hemorrhage, *Inflammation* 23, 461–469.
16. Barbaro, J. (2004) Design and Synthesis of Leukocyte Adhesion Inhibitors, *Curr. Org. Chem.* 8, 883–902.
17. Kogan, T. P., Dupre, B., Bui, H., McAbee, K. L., Kassir, J. M., Scott, I. L., Hu, X., Vanderslice, P., Beck, P. J., and Dixon, R. A. (1998) Novel synthetic inhibitors of selectin-mediated cell adhesion: synthesis of 1,6-bis[3-(3-carboxymethylphenyl)-4-(2-alpha-D-mannopyranosyloxy)phenyl]hexane (TBC1269), *J. Med. Chem.* 41, 1099–1111.
18. Kogan, T. P., Dupre, B., Keller, K. M., Scott, I. L., Bui, H., Market, R. V., Beck, P. J., Voytus, J. A., Revelle, B. M., and Scott, D. (1995) Rational design and synthesis of small molecule, non-oligosaccharide selectin inhibitors: (alpha-D-mannopyranosyloxy)biphenyl-substituted carboxylic acids, *J. Med. Chem.* 38, 4976–4984.
19. Davenpeck, K. L., Berens, K. L., Dixon, R. A., Dupre, B., and Bochner, B. S. (2000) Inhibition of adhesion of human neutrophils and eosinophils to P-selectin by the sialyl Lewis antigen TBC1269: preferential activity against neutrophil adhesion in vitro, *J. Allergy Clin. Immunol.* 105, 769–775.
20. Wang, L., Brown, J. R., Varki, A., and Esko, J. D. (2002) Heparin's anti-inflammatory effects require glucosamine 6-O-sulfation and are mediated by blockade of L- and P-selectins, *J. Clin. Invest.* 110, 127–136.
21. Koenig, A., Norgard-Sumnicht, K., Linhardt, R., and Varki, A. (1998) Differential interactions of heparin and heparan sulfate glycosaminoglycans with the selectins. Implications for the use of unfractionated and low molecular weight heparins as therapeutic agents, *J. Clin. Invest.* 101, 877–889.
22. Jain, R. K., Piskorz, C. F., Huang, B. G., Locke, R. D., Han, H. L., Koenig, A., Varki, A., and Matta, K. L. (1998) Inhibition of L- and P-selectin by a rationally synthesized novel core 2-like branched structure containing GalNAc-Lewisx and Neu5Acalpha2-3Galbeta1-3GalNAc sequences, *Glycobiology* 8, 707–717.
23. Galustian, C., Childs, R. A., Yuen, C. T., Hasegawa, A., Kiso, M., Lubineau, A., Shaw, G., and Feizi, T. (1997) Valency dependent patterns of binding of human L-selectin toward sialyl and sulfated oligosaccharides of Le(a) and Le(x) types: relevance to anti-adhesion therapeutics, *Biochemistry* 36, 5260–5266.
24. Kolbinger, F., Patton, J. T., Geisenhoff, G., Aenis, A., Li, X., and Katopodis, A. G. (1996) The carbohydrate-recognition domain of E-selectin is sufficient for ligand binding under both static and flow conditions, *Biochemistry* 35, 6385–6392.
25. Taylor, A. D., Neelamegham, S., Hellums, J. D., Smith, C. W., and Simon, S. I. (1996) Molecular dynamics of the transition from L-selectin- to beta 2- integrin-dependent neutrophil adhesion under defined hydrodynamic shear, *Biophys. J.* 71, 3488–3500.
26. Neelamegham, S., Taylor, A. D., Hellums, J. D., Dembo, M., Smith, C. W., and Simon, S. I. (1997) Modeling the reversible kinetics of neutrophil aggregation under hydrodynamic shear, *Biophys. J.* 72, 1527–1540.
27. Hentzen, E. R., Neelamegham, S., Kansas, G. S., Benanti, J. A., McIntire, L. V., Smith, C. W., and Simon, S. I. (2000) Sequential binding of CD11a/CD18 and CD11b/CD18 defines neutrophil capture and stable adhesion to intercellular adhesion molecule-1, *Blood* 95, 911–920.
28. Guyer, D. A., Moore, K. L., Lynam, E. B., Schammel, C. M., Rogelj, S., McEver, R. P., and Sklar, L. A. (1996) P-selectin glycoprotein ligand-1 (PSGL-1) is a ligand for L-selectin in neutrophil aggregation, *Blood* 88, 2415–2421.
29. Hemmerich, S., Leffler, H., and Rosen, S. D. (1995) Structure of the O-glycans in GlyCAM-1, an endothelial-derived ligand for L-selectin, *J. Biol. Chem.* 270, 12035–12047.
30. Tsurushita, N., Fu, H., Melrose, J., and Berg, E. L. (1998) Epitope mapping of mouse monoclonal antibody EP-5C7 which neutralizes both human E- and P-selectin, *Biochem. Biophys. Res. Commun.* 242, 197–201.
31. Nicholson, M. W., Barclay, A. N., Singer, M. S., Rosen, S. D., and van der Merwe, P. A. (1998) Affinity and kinetic analysis of L-selectin (CD62L) binding to glycosylation-dependent cell-adhesion molecule-1, *J. Biol. Chem.* 273, 763–770.
32. Somers, W. S., Tang, J., Shaw, G. D., and Camphausen, R. T. (2000) Insights into the molecular basis of leukocyte tethering and rolling revealed by structures of P- and E-selectin bound to SLe(X) and PSGL-1, *Cell* 103, 467–479.
33. Zhang, Y., and Neelamegham, S. (2002) Estimating the efficiency of cell capture and arrest in flow chambers: study of neutrophil binding via E-selectin and ICAM-1, *Biophys. J.* 83, 1934–1952.
34. Tsujishita, H., Hiramatsu, Y., Kondo, N., Ohmoto, H., Kondo, H., Kiso, M., and Hasegawa, A. (1997) Selectin-ligand interactions revealed by molecular dynamics simulation in solution, *J. Med. Chem.* 40, 362–369.
35. Leppanen, A., Mehta, P., Ouyang, Y. B., Ju, T., Helin, J., Moore, K. L., van Die, I., Canfield, W. M., McEver, R. P., and Cummings, R. D. (1999) A novel glycosulfopeptide binds to P-selectin and inhibits leukocyte adhesion to P-selectin, *J. Biol. Chem.* 274, 24838–24848.
36. Diacovo, T. G., Puri, K. D., Warnock, R. A., Springer, T. A., and von Andrian, U. H. (1996) Platelet-mediated lymphocyte delivery to high endothelial venules, *Science* 273, 252–255.
37. Davis, T. M., and Wilson, W. D. (2000) Determination of the refractive index increments of small molecules for correction of surface plasmon resonance data, *Anal. Biochem.* 284, 348–353.
38. Bruehl, R. E., Dasgupta, F., Katsumoto, T. R., Tan, J. H., Bertozzi, C. R., Spevak, W., Ahn, D. J., Rosen, S. D., and Nagy, J. O. (2001) Polymerized liposome assemblies: bifunctional macromolecular selectin inhibitors mimicking physiological selectin ligands, *Biochemistry* 40, 5964–5974.
39. Eggens, I., Fenderson, B., Toyokuni, T., Dean, B., Stroud, M., and Hakomori, S. (1989) Specific interaction between Le^x and Le^a determinants. A possible basis for cell recognition in preimplantation embryos and in embryonal carcinoma cells, *J. Biol. Chem.* 264, 9476–9484.
40. Seidler, J., McGovern, S. L., Doman, T. N., and Shoichet, B. K. (2003) Identification and prediction of promiscuous aggregating inhibitors among known drugs, *J. Med. Chem.* 46, 4477–4486.
41. Ruchaud-Sparagano, M. H., Malaud, E., Gayet, O., Chignier, E., Buckland, R., and McGregor, J. L. (1998) Mapping the epitope of a functional P-selectin monoclonal antibody (LYP20) to a short complement-like repeat (SCR 4) domain: use of human-mouse chimaera and homologue-replacement mutagenesis, *Biochem. J.* 332 (Part 2), 309–314.
42. Geng, J. G., Heavner, G. A., and McEver, R. P. (1992) Lectin domain peptides from selectins interact with both cell surface ligands and Ca²⁺ ions, *J. Biol. Chem.* 267, 19846–19853.
43. Revelle, B. M., Scott, D., and Beck, P. J. (1996) Single amino acid residues in the E- and P-selectin epidermal growth factor domains can determine carbohydrate binding specificity, *J. Biol. Chem.* 271, 16160–16170.

44. Kansas, G. S., Saunders, K. B., Ley, K., Zakrzewicz, A., Gibson, R. M., Furie, B. C., Furie, B., and Tedder, T. F. (1994) A role for the epidermal growth factor-like domain of P-selectin in ligand recognition and cell adhesion, *J. Cell Biol.* 124, 609–618.
45. Dwir, O., Kansas, G. S., and Alon, R. (2000) An activated L-selectin mutant with conserved equilibrium binding properties but enhanced ligand recognition under shear flow, *J. Biol. Chem.* 275, 18682–18691.
46. Mehta, P., Cummings, R. D., and McEver, R. P. (1998) Affinity and kinetic analysis of P-selectin binding to P-selectin glycoprotein ligand-1, *J. Biol. Chem.* 273, 32506–32513.
47. Wild, M. K., Huang, M. C., Schulze-Horsel, U., van der Merwe, P. A., and Vestweber, D. (2001) Affinity, kinetics, and thermodynamics of E-selectin binding to E-selectin ligand-1, *J. Biol. Chem.* 276, 31602–31612.
48. Jain, R. K., Vig, R., Locke, R. D., Mohammad, A., and Matta, K. L. (1996) Selectin ligands: 2,3,4-tri-O-acetyl-6-O-pivaloyl- α/β -galactopyranosyl halide as novel glycosyl donor for the synthesis of 3-O-sialyl or 3-O-sulfo Le^x and Le^a type structures, *Chem. Commun.* 1, 65–67.
49. Xia, J., Alderfer, J. L., Piskorz, C. F., and Matta, K. L. (2001) The 2-naphthylmethyl (NAP) group in carbohydrate synthesis: first total synthesis of the GlyCAM-1 oligosaccharide structures, *Chem. Eur. J.* 7, 356–367.
50. Liao, W., Piskorz, C. F., Locke, R. D., and Matta, K. L. (2000) N-p-nitrobenzyloxycarbonyl galactosamine imidate as a glycosyl donor for the efficient synthesis of mucin core-2 analogue, *Bioorg. Med. Chem. Lett.* 10, 793–795.

BI0507130